

Behaviour of Laterally Loaded Flexible Piles in Soft Clay

Azza Hassan Moubarak¹; Kamal Mohamed Hafez² and Karem Farouk Ibraheem³

¹Assistant Professor of Soil Mechanics and Foundation, Suez Canal University, Ismailia, Egypt

²Professor of Soil Mechanics and Foundation, Suez Canal University, Ismailia, Egypt

³Suez Canal Research Center, Suez Canal Authority, Ismailia, Egypt

azza_moubarak@eng.suez.edu.eg

Abstract: Behaviour of laterally loaded pile (LLP) requires accurate description for nonlinear performance of interaction between pile and the supporting soil. The encountered soil at East of Port-Said region is soft clay and extends down to more than fifty meters. In this study, available soil reports are reinterpreted to evaluate the required soil parameters. Concrete piles with different diameters are studied. Broms method is utilized to evaluate the ultimate lateral load (P_U) and maximum lateral ground deflection (y_{gmax}). Comparative study between different methods such as P-y method, non-dimension method (NDM) and finite element method (FEM) using Hardening Soil Model (HSM undrained) is accomplished to obtain LLP capacity. The results showed that PU (Broms method) used at this study as reference load to compare between other methods equals about $485D^2$ (kN), the average maximum bending moment for all methods equals about $1364D^{2.91}$ (kN.m) at ultimate load. The ultimate value (P_U) of the lateral load reached at the maximum lateral deflection (y_{gmax}) is about 7.5% of the pile diameter. Considering creep, the increase in percentage of (y_{gmax}) due to long term condition compared with short term ranges from 188% to 273% while the increase in percentage in maximum B.M. ranges from 31% to 57% according to pile diameter. Presence of pile cap relative to free head pile have a significant effect in reducing the maximum lateral deflection by about 38% and reducing the maximum bending moment by 41.75%.

[Azza Hassan Moubarak; Kamal Mohamed Hafez and Karem Farouk Ibraheem. **Behaviour of Laterally Loaded Flexible Piles in Soft Clay.** *Life Sci J* 2018;15(7):47-58]. ISSN: 1097-8135 (Print) /ISSN: 2372-613X (Online). <http://www.lifesciencesite.com>. 7. doi:10.7537/marslsj150718.07.

Keywords: Laterally loaded pile; Soft clay; Creep; Finite element method; Hardening soil model; Soft soil creep model

1. Introduction

The ability to reach reasonable estimation for the behaviour of laterally loaded piles is an important goal in this study. Lateral loads may represent about 10-15% of the vertical loads in case of on shores structures and about 25-30% in case of coastal and offshore structures [1]. For safe and economic pile foundation, pile behaviour should be assessed correctly, using pile load tests and /or well-known analytical methods. The Egyptian government has a plan for developing the East of Port-Said region which is located between $31^{\circ}14'$ to $31^{\circ}0'$ longitude and $32^{\circ}18'$ to 32° latitude by creating industrial and logistic zones where the international trade passing through Suez Canal as shown in Figure 1. Soft clay soil in this region extends to more than 50 m below the ground surface and is considered among the most problematic soils due to their low strength, high compressibility and time dependence of deformation. In this study the most common methods used to evaluate the lateral capacity of piles are:

- Broms Method (1964) [2].
- P-y Curve Method "Matlock 1970" [3].
- Non-Dimension Method (NDM) "Matlock and Reese, 1956" [4].
- Finite Element Method (FEM) [5].

This paper introduces the available soil reports done in the study area to determine the different soil parameters needed to calculate capacity of laterally loaded pile.

2 Geotechnical Site Properties

Available soil report (Pacer-Royal Haskoning-2006) [6] included an extensive field and laboratory studies had been carried out for the site. The results are reinterpreted in order to determine the engineering soil properties needed to evaluate the capacity of laterally loaded piles.

2.1 Stresses-Deformation Characterizations

One hundred and ninety unconsolidated undrained triaxial tests (UU) were included in geotechnical report [7]. Stress-strain curves were reinterpreted to investigate the values of deformation and strength parameters (modulus of elasticity of soil, E_S and undrained cohesion, C_U) of soil. The magnitude of E_S is related to the value of strain as shown in Figure 2 [8], with the largest value from a line that is tangent to the initial portion of the curve. The largest value of E_S called E_{Smax} or E_0 : initial modulus of elasticity, E_{50} : modulus of elasticity at strain = 50%. Reinterpretation of all UU tests using hyperbolic model (Duncan & Chang, 1970) [9] to

extract values of E_0 . These parameters E_0 , E_{50} and C_u are averaged and levelled at each depth and shown in Figure 3.

2.2 Modulus of Subgrade Reaction (K)

Carter, 1984[10] recommended a linear relationship between modulus of subgrade reaction and pile width by using appropriate parameters to describe the effect of the pile width on the subgrade reaction, as given by equation 1, [11].

$$K = \frac{1.0E_s D}{(1-\nu_s^2)D_{ref}} \left(\frac{E_s D^4}{E_p I_p} \right)^{1/12} \quad (1)$$

Where:

ν_s is the Poisson's ratio of the soil, D is pile diameter (m), D_{ref} equals 1.0 m, $E_p I_p$ is flexural rigidity of pile ($kN.m^2$), E_s is soil modulus of elasticity ($kN.m^2$).

The value of K with depth for a pile diameter with diameter 1.0 m is shown in Figure 4.

2.3 Variation of Soil Elastic Modulus (n_h) with Depth

The most useful form of variation of E_s with depth for normal consolidated clay is linear relationship and was expressed as follows [12].

$$E_s = n_h * \text{depth} \quad (2)$$

E_s : Modulus of soil elasticity

n_h : Variation of Modulus of soil elasticity with depth (h).

Figure 5 illustrates the variation of soil elastic modulus E_{50} (n_h) with depth, (n_h) for study area = 118 kN/m^3 .

2.4 Evaluation of Strain E_{50} :

E_{50} is defined as the percentage of strain corresponding to one-half the compressive strength of

the specimen at stress strain relationship Figure 6 shows variation of E_{50} with depth.

2.5 Unit Weight of Soil (γ) versus Depth:

The unit weight is plotted with depth as shown in Figure 7.

2.6 Plasticity Indexes

The plasticity index (PI %), liquidity index (LI), liquidity limit (LL %) and water content (W_C %) are plotted against the depth as shown in Figure 8.

The Summary of average geotechnical properties which concluded from the Geotechnical reports, are shown in Table 1.

3 Parametric Study

3.1 Analysis of Flexible Single Laterally Loaded pile

The capacity of flexible pile depends also on the capacity of pile section to resist bending moment. Broms method as traditional technique of limit analysis is used to evaluate the ultimate lateral load. The ultimate load calculated using Broms's method is used as reference load for other methods to compare between results.

Various flexible piles with diameters (0.5 m, 0.750 m, 1.0 m, 1.5 m) are chosen with fixed pile length 25 m. First short term load equals to Broms ultimate load is applied at the free pile head at the ground level.

3.2 Pile Properties

The pile used in this study is concrete bored pile with average compressive strength $f_{cu} = 250 \text{ kg/cm}^2$. The relation between E_p and f_{cu} is expressed as follows:

$$E_p = 14000 (f_{cu})^{0.5}, E_p = 2.2 * 10^7 \text{ kN/m}^2$$

Table 1: Summary of the average geotechnical properties of soil at East of Port-Said (EGYPT)

Depth(m)	Soil type	C_u (Kpa)	E_f (Kpa)	$E_{50\%}$ (Kpa)	ν_{50}	γ (kN/m^3)	K (kN/m^2)	n_h (kN/m^3)	LL %	W.C %	PI %	LI	q_{ult} (KPa)
0 ~ 5	Clay with high plasticity (CH)	33.6	4770	2690	3.05	18.2	2820		45.4	28.2	23.3	0.57	84.8
5 ~ 10		13.9	4890	2840	1.70	16.2	2970		61	37	34.2	0.86	30.2
10 ~ 15		9.6	1695	760	2.86	15.2	710		56.3	55.3	29.3	1.11	20.8
15 ~ 20		48.3	7070	3125	2.01	17.1	3325		51.7	57.9	27.1	0.91	144.6
20 ~ 25		26.4	5300	3100	1.17	16.5	3260		65.7	48.9	38	0.80	58.8
25 ~ 30		30.1	6390	2900	0.88	16.2	3050		69.7	58.2	41.5	0.77	65.8
30 ~ 35		27.3	7580	3050	0.8	15.7	3250	170	73.9	61.3	42.9	0.82	58.7
35 ~ 40		27.6	5035	2600	0.71	16.2	2700		88.2	62.9	51.9	0.59	59.3
40 ~ 45		35.1	12740	3100	0.71	16.0	3260		90.7	65.7	56.2	0.54	79.8
45 ~ 50		27.5	16095	6275	0.42	15.6	7200		92.8	64.9	57.5	0.61	67.5
50 ~ 55		34.8	9795	4870	0.4	15.9	5320		97.7	69.5	59.9	0.52	79.5
55 ~ 60		43.9	21050	8970	0.47	16.3	10390		107	68.8	56.4	0.52	81.5

Table 2: Capacity of pile section to resist bending moment

D (m)	0.5	0.75	1	1.5
A _S (cm ²)	29.5	66.5	118	265
M _U (kN.m)	156	527	1250	4220

γ_p , is the unit weight of concrete = 24 kN/m³, ν_p : Poisson's ratio of concrete = 0.15, according to the pile section with reinforcement ratio =1.5% and vertical load = 0 kN the interaction diagrams used to evaluate the ultimate bending moment capacity for pile (M_U) kN.m are given in Table 2.

4 Analysis and Results

4.1 Capacity of Pile using Broms Method

Broms presented a set of curves and equations for solving the problem of long flexible pile, depending on head condition of pile (fixed or free) and some parameters as M_U, C_U and pile diameter D. The results are shown in Table 3.

Table 3: capacity of pile using Broms method

D (m)	0.5	0.75	1.0	1.5
$B = \left(\frac{K_h * D}{4E_p * I_p}\right)^{\frac{1}{4}} (m^{-1})$	0.271	0.2003	0.1609	0.1187
$E_p * I_p (kN.m^2) * 10^3$	67.5	341.8	1080.4	5469.3
M _U (kN.m)	156	527	1250	4220
P _U (kN)	122	273	485	1090
y _g max. (cm)	4.6	5.0	5.4	6.0

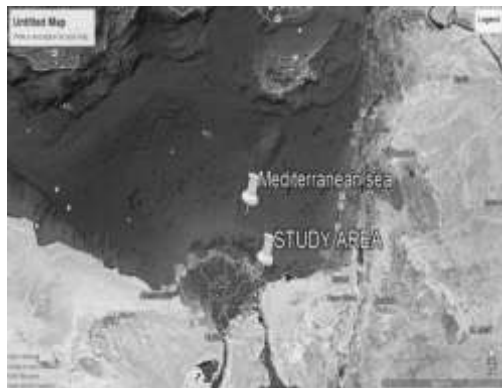


Fig.1 Suez Canal site

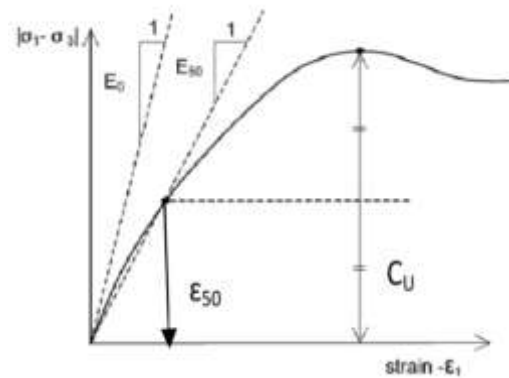


Fig.2 Stiffness modulus of soil

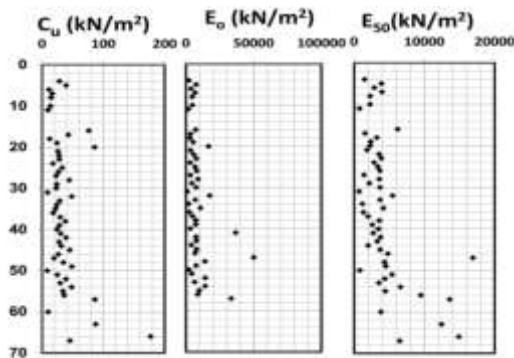


Fig.3 Shear cohesion (c_u) and deformation parameters of soil, E_O, and E₅₀ with depth (m)

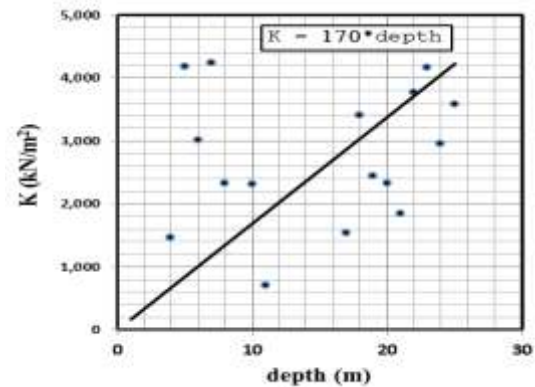


Fig.4 Variation of soil subgrade reaction K with depth at pile diameter 1.0m

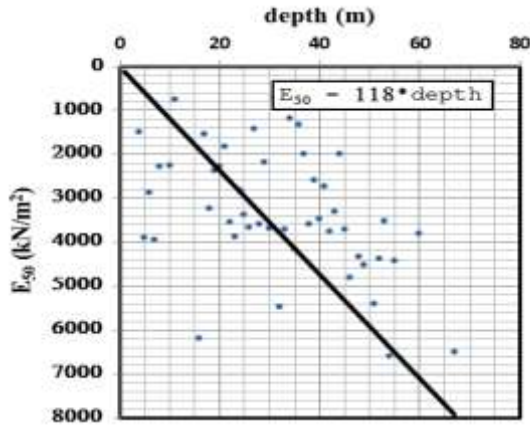


Fig.5 Variation of Elastic modulus of soil (E_{50}) with depth

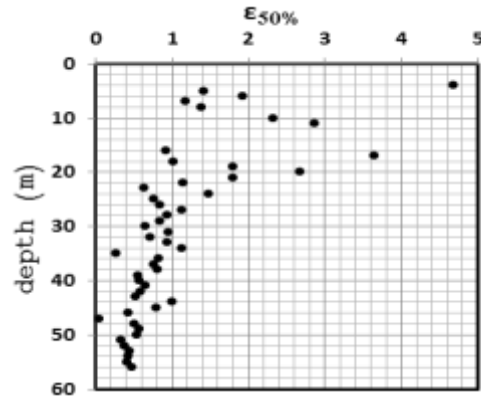


Fig.6 Variation of (ϵ_{50}) with depth

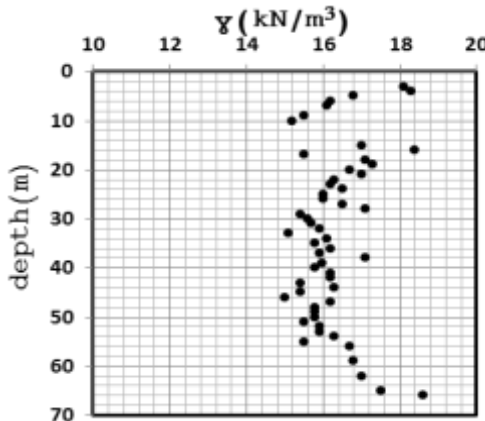


Fig.7 Variation of unit weight with depth

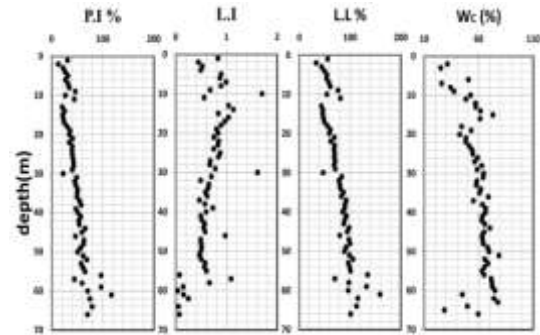


Fig.8 Variation of plasticity indexes with depth

Figure 9, shows the relation between pile diameter D (m) and the ultimate load P_U (kN) Figure 10, shows the relation between D (m) and y_{gmax} (cm), where K_n : coefficient of subgrade reaction (kN/m^3), β ; relative stiffness, I_p ; pile inertia, y_{gmax} ; maximum deflection of pile at ground level due to ultimate load (P_U).

4.2 Capacity of Laterally Loaded Pile using p-y Curves Method

The method depends on how exactly the mobilization of soil reaction versus a laterally loaded pile is represented. The model proposed by (Matlock-1970) [3] is widely used and applied for soft clay soil. It depends on the best possible estimate of the

variation of undrained shear strength C_U , value of E_{50} and submerged unit weight (γ) with depth.

The curves of P - y were derived at the different depths (h) for diameters of piles (D) = 0.5, 0.75, 1.0, 1.5 m. **ALLPILE** program version 6.5 was used to solve the soil-structure interaction equilibrium problem. Table 4 shows the values of P_U , y_{gmax} , normalized location of max B.M along the length of pile.

Figure 11a and Figure 11b show the relation between the deflection and the maximum bending moment on piles using p - y curve methods for different D . Figure 11b, shows that whenever the pile diameter increase (pile flexibility decreases) the length of pile which is encased by bending moment increases.

Table 4: value of y_{gmax} , B.M_{max}, location of max B.M along pile (p-y method)

D (m)	0.5	0.75	1.0	1.5
P_u (kN)	122	273	485	1090
y_{gmax} (cm)	3.8	7	10.6	22.3
B.M max. (kN.m)	164	593	1460	4710
Normalize depth of max. B.M to the total length	0.120	0.192	0.272	0.372

4.3 Capacity of Laterally Loaded Pile using Non-Dimensional Method (NDM)

The physical character of soils led to E_{py} : modulus reaction for a pile under lateral loading should be zero at the mud line and increase linearly with depth $E_{py} = K_{py} \cdot \text{depth}$, where K_{py} : coefficient of subgrade reaction for pile [13].

Matlock and Reese (1960) [14] introduced equations for determining the bending moment and deflection at any point along the pile length.

Table 5 shows the values of P_U , y_{gmax} , max. B.M and the location of max. B.M. normalized to total length of pile.

The relation between the deflection and the maximum bending moment of piles using NDM method for different pile diameters are shown in Figure 12a and Figure 12b.

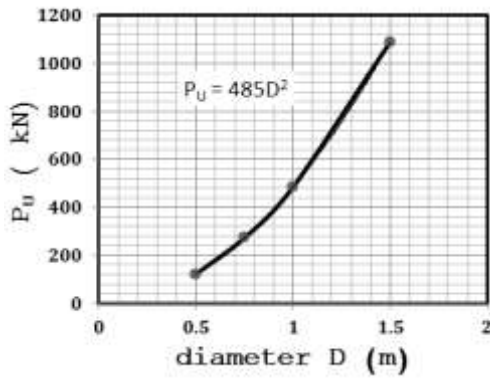


Fig.9 Effect of Diameter variation on P_u

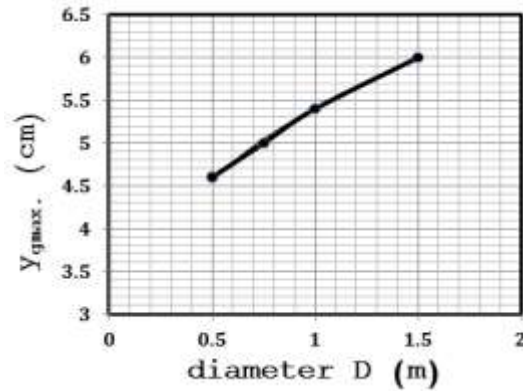


Fig.10 Effect of variation of diameter on max lateral deflection

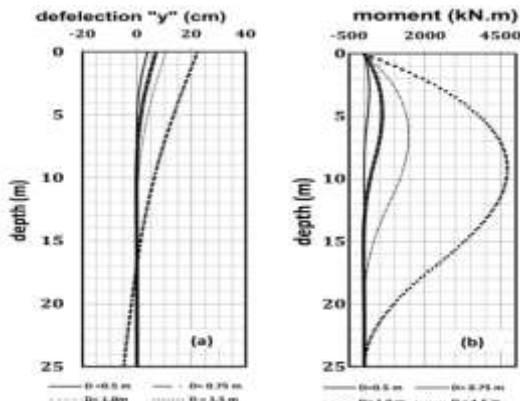


Fig.11 Deflection and Bending moment (P - y) method

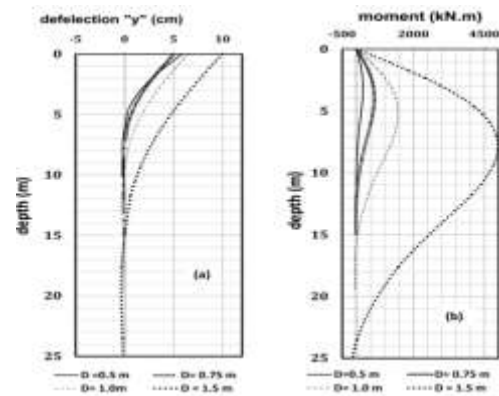


Fig.12 (a,b) Deflection and Bending moment (NDM)

Table 5: Value of y_{gmax} , B.M max, location of max B.M along pile (NDM)

D (m)	0.5	0.75	1	1.5
P_u (kN)	122	275	485	1090
y_{gmax} (cm)	5.86	5.03	6.48	10
B.M max. (kN.m)	223	626.3	1460	4964
Normalize depth of max. B.M to the total length	0.132	0.168	0.220	0.332

4.4 Capacity of Laterally Loaded Piles using Finite Element Method (FEM)

Finite element package, Plaxis 3D foundation [5] was used to calculate the capacity of single free head pile. The pile is modelled using an embedded pile model which is available in Plaxis 3D. The model geometry has been created with dimensions of 40 m in both X, Z directions and 45 m in y direction as shown in Figure 13. The soil profile has 9 layers according to Table 1.

The model is implemented with fine mesh coarseness and number of elements = 10584. The

constitutive model of port-said clay is represented by the hardening soil model (HSM). The hardening-soil model is an advanced model for simulating the behaviour of different type of soils, soft soils and stiff soils, Schanz and Vermeer [15].

The parameters (drained and undrained) of HSM were summarized in Table 6 (Hamed et al) [16].

Summary of lateral pile capacity is shown in Table 7. In addition to, the response of piles for different diameters using FEM method (Plaxis 3D program) is shown in Figure 14.

Table 6: Summary of the HSM parameters after Hamed et al. (2017) [16]

layer	c'	ϕ'	$E_{u50}^{ref} (MPa)$	$m_{undrained}$	$E_{d50}^{ref} (MPa)$	$m_{drained}$	$E_{oed}^{ref} (MPa)$
clay	0	22	4.66	0.81	3.21	0.59	2.1

Table 7: y_{gmax} and B.M max using FEM (HSM-undrained parameters)

D (m)	0.5	0.75	1	1.5
Pu (kN)	122	275	485	1090
y_{gmax} at G.L (cm)	3.7	4.5	5.8	6
Max. B.M (kN.m)	209	565	1454	3954
Location of max. B.M from G.L (m)	2.5	2.5	5.0	5.0

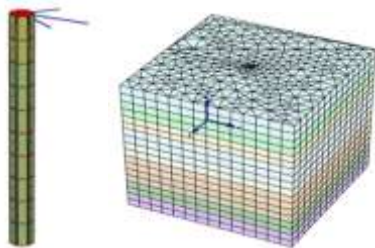


Fig.13 Finite element model (Plaxis 3D)

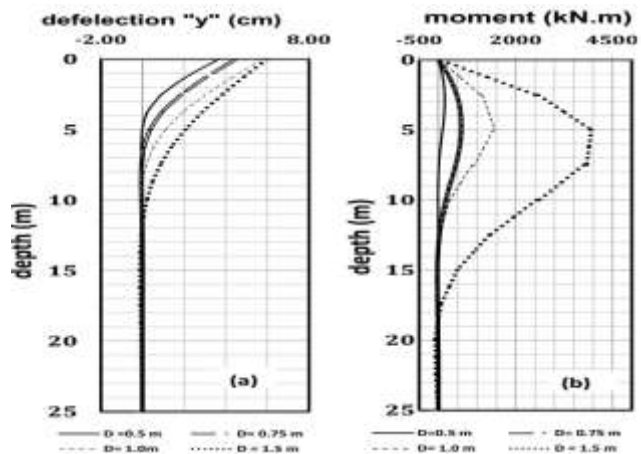


Fig.14 Deflection and Bending moment (FEM)

5 Effect of Creep on Laterally Loaded Pile

Bowles [17] mentioned that the lateral displacement from long-term Loading, produce secondary consolidation or creep, has not been much addressed for lateral piles. Kuppusamy and Buslov [18] gave some suggestions but still the parameters needed for the necessary equations were difficult to obtain.

The constitutive models of port-said clay were represented by two models, the hardening soil model (HSM) with drained parameters which are included in Table 6. The Soft Soil Creep Model (SSCM) is used

in order to quantify the contribution of secondary consolidation in the long-term conditions to the total deformation.

SSCM is used to simulate the long-term behaviour and it offers an additional advantage over the HSM by accounting for secondary consolidation effect as it significantly contributes the overall deformation of soft soils.

Results of one-dimensional consolidation tests given by Hamed et al [16], are used to determine the different SSCM parameters of Port-Said Clay as shown in Table 8.

Table 8: Summary of SSCM design parameters for Port-Said Clay (after Hamed et al.2017)

C_c	C_s	C_α	k^*	λ^*	μ^*	e_o	C'	ϕ'
0.75	0.105	0.014	0.03	0.109	0.002	2	0	22

Where: C_c : compression index, C_s : swelling index, C_α : coefficient of secondary consolidation, e_o : initial void ratio, k^* : modified swelling index, λ^* : modified compression index, μ^* : modified creep index, C' and ϕ' : effective shear strength parameters.

$$\lambda^* = \left(\frac{c_c}{2.3(1+e_o)} \right) (3)$$

$$k^* = \left(\frac{2c_s}{2.3(1+e_o)} \right) (4)$$

$$\mu^* = \left(\frac{C_\alpha}{2.3(1+e_o)} \right) (5)$$

5.1 Results of Creep

The maximum deflections at ground level (y_{gmax}) under ultimate lateral load at different diameters for different constitutive models are shown in Table 9.

The percentage of increase of y_{gmax} due to applying the HSM drained model (long term condition), SSCM which represent long term condition including creep also compared with HSM undrained (short term condition) are shown in Table 10 and Figure 15. The percentage of increase of (y_{gmax}) due to creep ranges from 188% to 273%, while the percentage of increase in maximum B.M. ranges from 31% to 57% corresponding to variation of pile diameters.

Table 9: Results of max. Deflection y_{gmax} for piles using HSM and SSCM

Ultimate Load (kN)	Diameter (m)	Deflection y_{gmax} Using HSM. (cm)		Using SSCM (cm)
		Undrained	Drained	
120	0.5	3.7	6.4	13.8
270	0.75	4.5	7.5	15.2
485	1.0	5.8	8.6	16.7
1090	1.5	6.0	9.8	18.1

Table 10: Percentage of increase of y_{gmax} due to HSM (drained) and SSCM comparing with HSM (undrained)

% increase of y_{gmax} for pile diameter (FEM) compared with HSM undrained					
Diameter (m)	0.5	0.75	1.0	1.5	Average %
HSM (drained)	73	67	48	63	62.5
SSCM (drained)	273	238	188	200	230

Kuppusamy and Buslov [18] shows a comparison between creep deflection calculated by finite element method and field test data. It can be seen that the elastic deflections are relatively less than creep deflections and that the percentage of increase of creep deflection relative to elastic deflection reaches 575% as shown in Figure 16.

The results of maximum bending moment due to ultimate lateral load for piles with different diameters

using different constitutive models are shown in Table 11. It is noticed that the percentage of increase of maximum bending moment due to HSM (in drained condition) and SSCM compared with HSM (undrained condition) are shown in Table 12 and Figure 17. The percentage of increase of max. B.M due to creep ranges from 31% to 57% compared with short term condition as shown in Figure 17.

Table 11: Max. B.M on piles using HSM and SSCM

Ultimate Load (kN)	Pile Diameter (m)	Max. B.M. using HSM. (cm)		Max. B.M using SSCM kN.m
		undrained	Drained	
120	0.5	209	226	284
270	0.75	565	675	885
485	1.0	1450	1530	1900
1090	1.5	3950	4540	5570

Table 12: Percentage of increase of max B.M due to HSM and SSCM compared with HSM

% increasing at max B.M with pile diameter compared with HSM undrained					
Diameter (m)	0.5	0.75	1.0	1.5	Average %
HSM (drained)	8	19	6	16	12
SSCM (drained)	36	57	31	41	41

6 Comparison between Different Methods

The values of maximum ground deflection (y_{gmax}) calculated by different methods in short term condition are shown in Table 13. Figure 18 shows the relationship between the pile diameter and y_{gmax} , it can be observed that the large variation between maximum ground deflections calculated by the four different

methods range from 100% to 370% compared with that calculated value by Broms method.

Also, the values of max bending moment calculated by different methods are shown in Table 14. Figure 19 shows the relationship between pile diameter and max B.M. calculated by the four different methods compared with that calculated value by Broms method, it ranges from 94% to 119%.

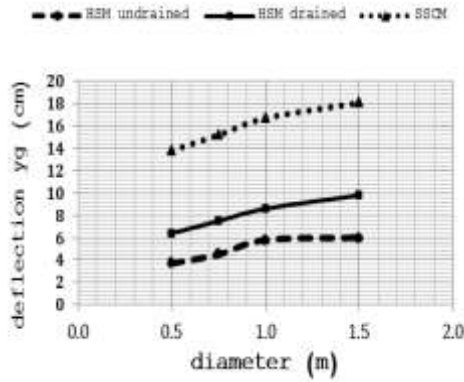


Fig.15 Deflection y_{gmax} using HSM and SSCM

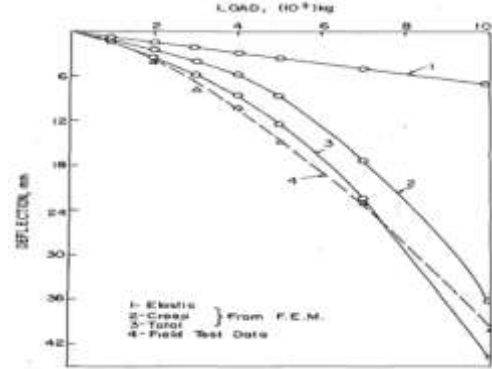


Fig.16 Relation between load and deflection after Kuppusamy and Buslov 1987 [18]

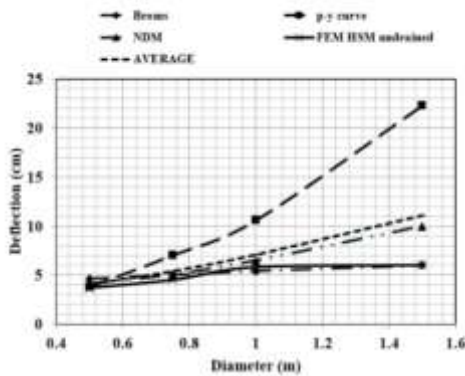


Fig.17 Max Bending moment using HSM (undrained), HSM (drained) and SSCM

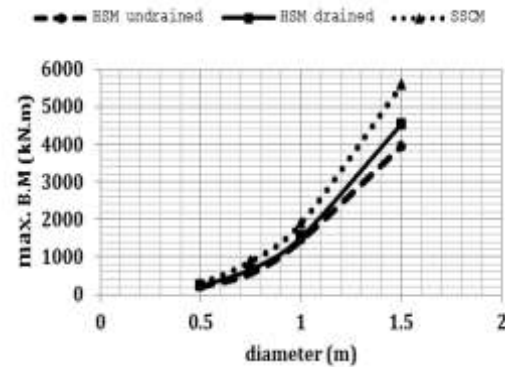


Fig.18 Values of y_{gmax} using different methods

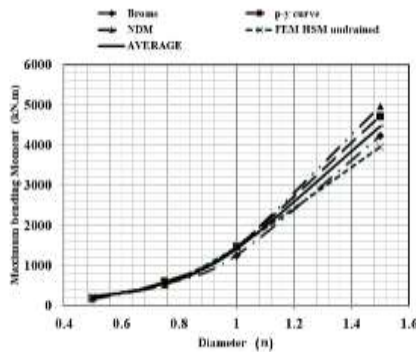


Fig.19 Values of max Bending moment using different methods

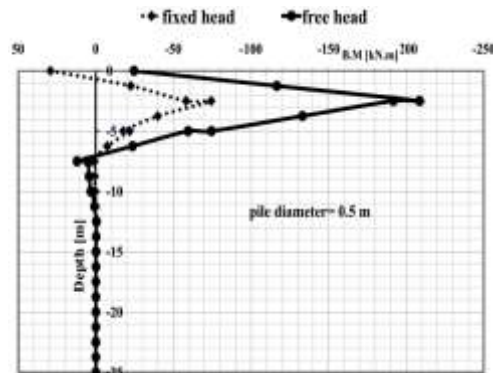


Fig.20 Bending moment at D=0.5 m

Table 13: Max deflection y_{gmax} using different methods

Deflection y_{gmax} on pile with Broms -ultimate load P_u (kN)				
Diameter (m)	0.50	0.75	1.0	1.5
P_u (kN)	122	273	485	1090
Broms Method	4.6	5	5.4	6
P-y curve Method	3.8	7.0	10.6	22.3
NDM Method	4.1	5.0	6.5	10
Finite Element Method- HSM	3.7	4.5	5.8	6
Average	4.1	5.4	7.1	11.1

Table 14: Max Bending Moment (B.M) using different methods

Max. Bending Moment (kN.m) on pile with Bromsultimate load P_u (kN)				
Diameter (m)	0.5	0.75	1.0	1.5
P_u (kN)	122	273	485	1090
Broms Method	156	527	1250	4220
P-y curve Method	164	593	1460	4710
NDM Method	223	526	1460	4964
Finite Element Method - HSM	209	565	1454	3954
Average	188	553	1406	4462

7Effect of Pile cap

When the pile head has a cap the values of the B.M along the pile length are affected. Figures 20 to 23 show the values of the bending moment distributed along the pile length at different pile diameters for free and fixed head. Figures 24 to 27 indicate that the values of the deflection along the pile length for free pile and pile with cap at different pile diameters. Table 15 shows the maximum values of the head pile deflection and the bending moment for free head and pile with cap at different pile diameters. The

percentages of reduction at ground deflection and maximum bending moment along pile length were illustrated at Table 15.

8Effect of Pile Cap Thickness (foundation thickness)

Figure 28 shows the values of the bending moment at the pile head for different pile diameters and different pile cap thickness. It can be observed that the thickness of pile cap has no significant effect on the bending moment at the pile head.

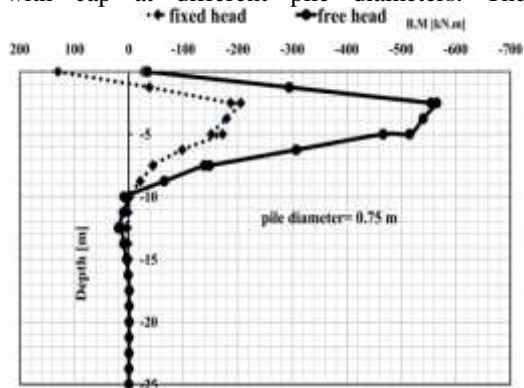


Fig.21 Bending moment at D=0.75 m

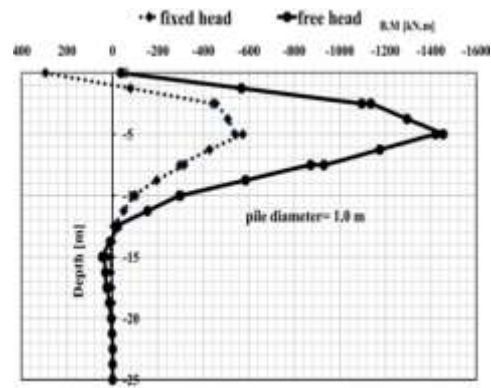


Fig.22 Bending moment at D=1.0m

Table 15: Maximum value of head deflection and bending moment for free head and pile with cap

Pile diameter [m]	Free head condition			Pile with cap head condition			% ground deflection (with cap/free) (B/A)	% Max. B.M (with cap/free) (C/D)
	{A} Ground deflection [cm]	B.M max. [kN.m]		{B} Ground deflection [cm]	B.M max. [kN.m]			
		Top B.M	Along pile {D}		Top B.M	Along pile {C}		
0.5	3.8	-	212.7	1.14	29.3	74.4	0.30	0.35
0.75	4.6	-	572	1.50	130.2	205.5	0.32	0.36
1.0	5.7	-	1450	2.10	295	573	0.37	0.40
1.5	6.0	-	3960	3.35	942.3	2212	0.56	0.56

9. Effect of pile length on the ground line deflection

Figure 29(a, b), show that there will be a significant increase in the ground line deflection as the pile length is less than critical. The length of pile must be selected to give an appropriate factor of safety against excessive ground line deflection (Reese and Van Impe 2001) [19].

Figure 30 shows the relation between pile length and ground line deflection for pile diameters equal

(0.5, 0.75, 1 and 1.5 m) at study area. It is noticed that the critical length of piles are given as ratio of pile diameter. Table 16 shows the values of the critical length /diameter of the pile are approximately close to 12 for all diameters. This means that any increase in pile length more than the critical length of the pile has no effect in decreasing the lateral deflection of the pile.

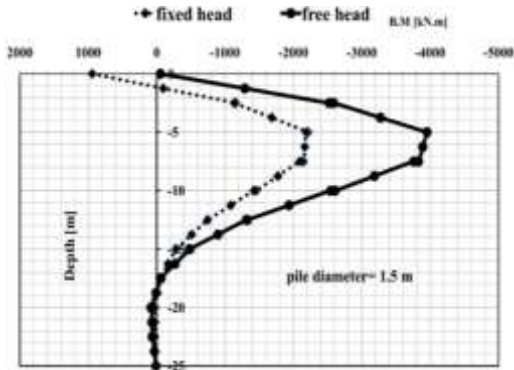


Fig.23 Bending moment at D=1.5m

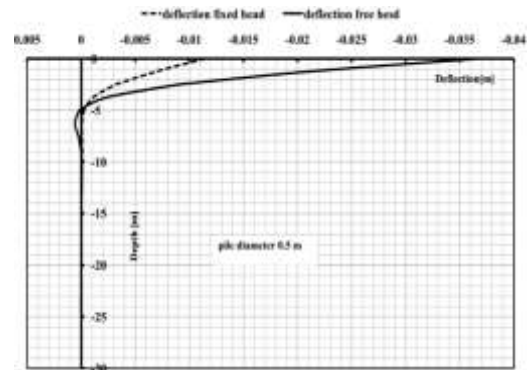


Fig. 24 Deflection (m) at D=0.5m

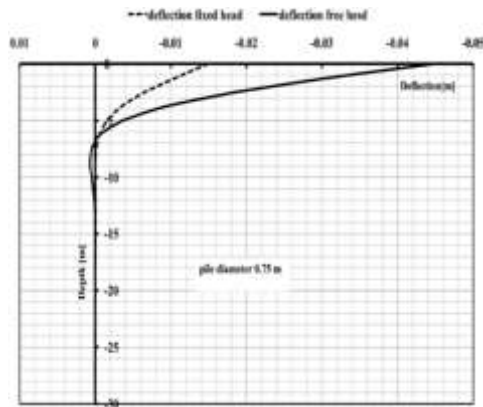


Fig.25 Deflection (m) at D=0.75m

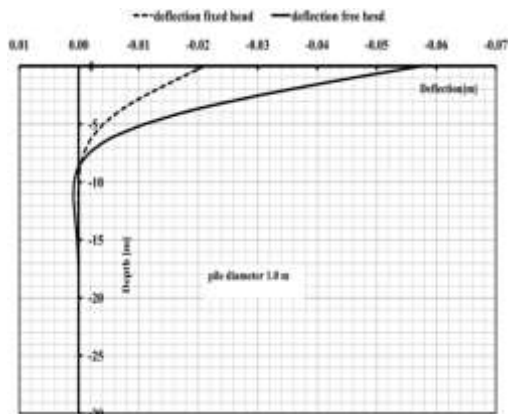


Fig.26 Deflection (m) at D=1.0m

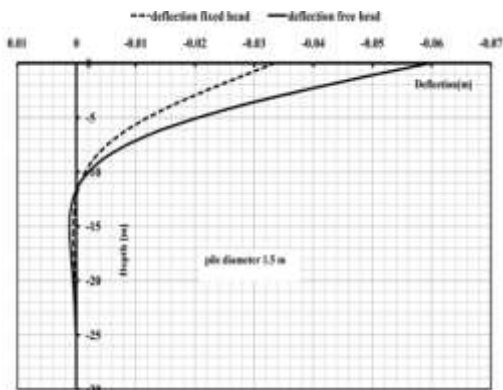


Fig. 27 Deflection (m) at D=1.5m

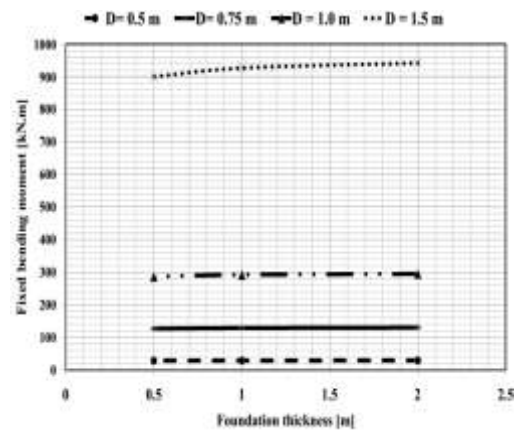


Fig.28 Effect of pile cap thickness (foundation thickness)

Table 16: Values of critical length of pile at different pile diameters

Pile Diameter's "D" (m)	0.5	0.75	1.0	1.5
Critical Length "L _{crit} " (m)	6.0	9.0	12	15
L _{crit} /D	12	12	12	10
βL_{crit}	1.62	1.80	1.93	1.78

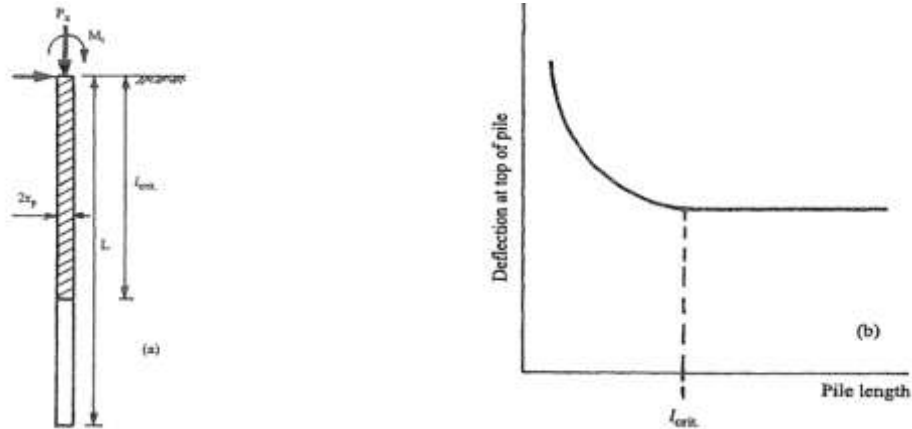


Fig. 29 (a , b) Critical Pile length (Reese and Van Impe 2011) [19]

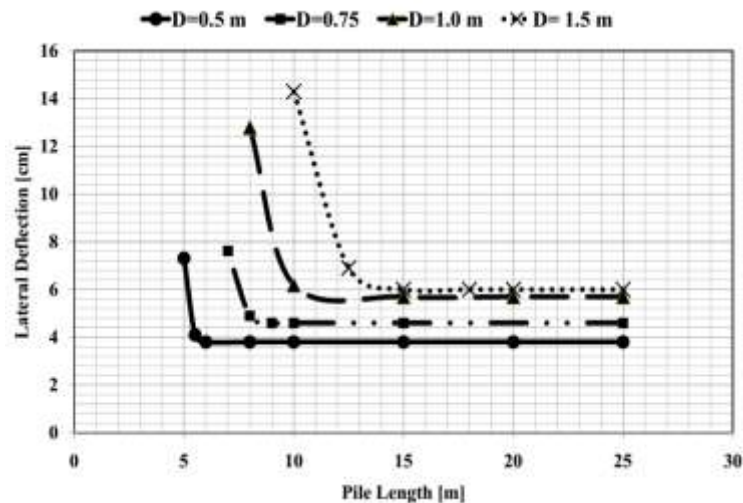


Fig. 30 Relation between pile length and ground deflection with different pile diameters

10. Conclusion

Based on this research the following conclusions are drawn:

- The ultimate load of laterally loaded pile in soft clayey soil can be represented by the equation $P_u = 485D^2$ kN, while the average maximum bending moment can be represented by the equation $B.M_{max} = 1364D^{2.91}$ at ultimate load.
- Broms method gives very good estimation for the maximum deflection at pile head for flexible pile at soft clay when compared with other methods.
- P-y method gives highly estimation for deflection at pile head for flexible pile in soft clay especially for large diameter pile, but it gives good

estimation for the maximum bending moment when compared with other methods.

- Non-dimension method (NDM) gives very good estimation for both deflection at pile head and for the maximum bending moment along the pile when compared with other methods.

Finite element methods (FEM) using Hardening Soil Model (HSM undrained) for short term condition gives very good estimation for pile head deflection but give very low estimation for maximum bending moment along pile length when compared with other methods.

- Attention should be paid to study the effect of creep when the laterally loaded piles are

constructed in soft clay soils, especially when lateral displacement is governed by a limit value, as creep increases the lateral displacement increases by 188% to 273% relative to elastic displacement (short term displacement) while the increase in percentage in maximum B.M. ranges from 31% to 57% according to pile diameter.

- The value of ultimate lateral load occurs when the lateral displacement at ground level y_{gmax} around approximately to 7.5% of pile diameter for short-term loading HSM (undrained) model, while Arulanantham [20] and Sawwaf [21] mentioned that the ultimate lateral load occurs when y_{gmax} is around 10% of the pile diameter.

- Increase of pile length greater than critical length (12D) has no significant effect in decreasing the lateral deflection of laterally loaded pile.

- Considering laterally loaded pile with cap reduces the lateral deflection by about 38% and reducing the maximum bending moment by 41.75%. However, increasing the pile cap thickness trivially affects the lateral deflection and the maximum bending moment.

References

1. Chandrasekaran SS, Boominathan A. and Dodagoudar GR. (2009). Group interaction effects on laterally loaded piles in clay. *Journal of geotechnical and environmental engineering*, 136(4), 573-582.
2. Broms, Bengt B. (1964). Lateral resistance of piles in cohesive soils. *Proceedings of the American Society of Civil Engineers, Journal of the Soil Mechanics and Foundations Division*, vol. 90, SM2, 27-64.
3. Matlock H. (1970). Correlations for design of laterally loaded piles in soft clay. *Offshore Technology in Civil Engineering's Hall of Fame Papers from the Early Years*, 77-94.
4. Matlock H. and Reese LC. (1956). Non-dimensional solutions for laterally loaded piles with soil modulus assumed proportional to depth. *Association of Drilled Shaft Contractors*.
5. Plaxis Manual, "Plaxis 3D Foundation Material Models Manual version 1.5".
6. East Port Said Container Terminal Phase II East PORT-SAID Prepared by: Geogroup Geotechnical Consultant (Consultants: Pacer-Royal Haskonong) May 2006.
7. Smith TD. (1987). Pile horizontal soil modulus values. *Journal of Geotechnical Engineering*, 113(9), 1040-1044.
8. J. Michael Duncan, Andrew Bursey, Soil Modulus Correlations, *Foundation Engineering in the face of uncertainty*, ASCE 9/8/2013, p. 321-336.
9. Duncan JM. and Chang CY. (1970). Nonlinear analysis of stress and strain in soils. *Journal of Soil Mechanics & Foundations Div.*
10. Carter DP, (1984). A nonlinear soil model for predicting lateral pile response: Report 359. Technical report, University of Auckland.
11. Ashford SA., and Juirnarongrit T., (2003). Evaluation of pile diameter effect on initial modulus of subgrade reaction. *Journal of Geotechnical and Geoenvironmental Engineering*, 129(3), 234-242.
12. Smith, T.D. (1987). Pile horizontal soil modulus values. *Journal of Geotechnical Engineering*, 113(9), 1040-1044.
13. Goh ATC, Teh C I and Wong K.S. (1997). Analysis of piles subjected to embankment induced lateral soil movements. *Journal of geotechnical and Geoenvironmental Engineering*, 123(9), 792-801.
14. Matlock H and Reese LC (1960). Generalized solutions for laterally loaded piles. *Journal of the Soil Mechanics and foundations Division*, 86(5), 63-94.
15. Schanz T and Vermeer PA (1998). On the stiffness of sands. *Géotechnique*, 48, 383-387.
16. Hamed O, Mansour M, Abdel-Rahman A. and El-Nahas F. (2017). Investigating the Behaviour of an Existing Quay Wall Using the Characteristic Parameters of Port-Said Clay, Egypt, *World Applied Sciences Journal* 35(3): 483-499.
17. Bowles JE (1996), *Foundation Analysis and Design* Fifth Edition, the McGraw-Hill Book Company, Inc.
18. Kuppasamy T. and Buslov A. (1987). Elastic-creep analysis of laterally loaded piles. *Journal of geotechnical engineering*, 113(4), 351-365.
19. Reese LC. and Van Impe WF. (2011). *Single piles and pile groups under lateral loading*, CRC Press, Boca Raton, FL.
20. Arulanantham J (2015). 3-D finite element analysis of laterally loaded short shafts in soil. Thesis (master). Toronto, Ontario, Canada.
21. Sawwaf ME. (2006). Lateral resistance of single pile located near geosynthetic reinforced slope. *Journal of geotechnical and geoenvironmental engineering*, 132(10), 1336-1345.

7/24/2018